

N O T I C E

THIS DOCUMENT HAS BEEN REPRODUCED FROM
MICROFICHE. ALTHOUGH IT IS RECOGNIZED THAT
CERTAIN PORTIONS ARE ILLEGIBLE, IT IS BEING RELEASED
IN THE INTEREST OF MAKING AVAILABLE AS MUCH
INFORMATION AS POSSIBLE

NASA Technical Memorandum 81487

EFFECT OF INFLOW CONTROL ON
INLET NOISE OF A CUT-ON FAN

Richard P. Woodward and Frederick W. Glaser
Lewis Research Center
Cleveland, Ohio

Prepared for the
Sixth Aeroacoustics Conference
sponsored by the American Institute of Aeronautics and Astronautics
Hartford, Connecticut, June 4-6, 1980

EFFECT OF INFLOW CONTROL ON INLET
NOISE OF A CUT-OFF FAN

Richard P. Woodward and Frederick W. Glaser
National Aeronautics and Space Administration
Lewis Research Center
Cleveland, Ohio 44135

Abstract

A cut-on, high tip speed fan stage was acoustically tested with three configurations of an inflow control device in the NASA Lewis anechoic chamber. Although this was a cut-on design, rotor-inflow interaction appeared to be a much stronger source of blade passing tone radiated from the inlet than rotor-stator interaction for the 1.6 mean rotor chord separation. An external suction applied to the area where the inflow control device joins the inlet produced a further reduction in blade passing tone suggesting that disturbances in the forward flow on the outside of the inlet were superimposed on the inlet boundary layer and were a significant source of tone noise.

1. Introduction

Differences between turbofan noise levels measured in flight and in ground static tests have been well-documented in the literature (e.g., see Ref. 1). Noise studies performed in an anechoic wind tunnel have shown results similar to those obtained in flight tests.² Hanson³ has theorized that elongated turbulence eddies entering the fan inlet during static testing are responsible for the increased fundamental blade passing tone noise observed in these tests. Thus, it is necessary to control turbulence and other inflow disturbances in static turbofan noise studies to reveal noise generating mechanisms which would otherwise be masked by inflow disturbance induced noise. A number of inflow control devices, which have been tested and reported in the literature, showed varying success in reducing the fan blade passing tone levels (e.g., see Ref. 4 to 7).

In the present study, the inflow control device (ICD) of Ref. 4 and two modifications of it were tested on a fan model in the Lewis anechoic chamber. These inflow control studies were performed as part of a larger acoustic evaluation of this fan.

The fan did not have a sufficient number of stator vanes to cut off the rotor-stator interaction tone at blade passing frequency. Although a cut-off design would have been more desirable for isolating blade passing tone noise mechanisms in an inflow control study, earlier results from the Lewis anechoic chamber showed that rotor-inflow interaction could control tone generation even for a cut-on fan if the rotor-stator spacing is large enough. In the earlier study (see Ref. 4), the basic configuration of the ICD was tested in both cut-on and cut-off configurations. The minimum rotor-stator spacing on this fan was 1.5 mean rotor chords. These earlier tests showed the blade passing tone level to be controlled by inflow disturbances interacting with the rotor, rather than rotor-stator interaction, even with the cut-on configuration, suggesting that inlet fan noise in static testing is largely due to in-

flow disturbances for sufficient rotor-stator spacing. The present experiments provide a further check on this point as well as exploring possible refinements in the ICD construction.

II. Apparatus and Procedure

Anechoic Chamber

The results presented herein were obtained in the NASA Lewis anechoic chamber, which is described in detail in Ref. 8. Figure 1 is a photograph of the research fan installed in the anechoic chamber without the inlet flow control device. Plan and elevation views of the facility are given in Figs. 2(a) and (b). Calibration of the chamber showed it to be anechoic to within 2 dB for frequencies above 200 Hz. The chamber may be operated in either a "muffler open" mode in which the airflow primarily enters through the silencer, or in an aspirating mode in which the silencer is closed and air enters the chamber through aspirating areas on the chamber floor and walls. All of the results presented herein are for the muffler open mode of chamber operation.

Research Fan

The test fan used in this study was designed and fabricated by AirResearch Manufacturing Company of Arizona as a 50.8 cm (20 in.) tip diameter scale model of a 73.0 cm (28.7 in.) fan which they had built and tested earlier under contract to NASA-Lewis. Details of this fan stage design may be found in Ref. 9. Reference 10 presents aerodynamic and acoustic performance of the model fan stage in the Lewis anechoic chamber. The design rotor tip speed of this fan of 488 m/sec (1600 ft/sec) results in a blade relative Mach number equal to one at slightly greater than 60% design fan speed. The design stage pressure ratio was 1.5. The rotor-stator separation was 1.63 mean rotor chords.

The research fan had sufficient aerodynamic instrumentation to establish the operating point in terms of pressure ratio and mass flow. This instrumentation included inlet thermocouples and static pressure sensors for inlet mass flow calculations, and total temperature and pressure rise measurements across the stage. These measurements were processed through a pressure multiplexing network and computer system to calculate aerodynamic parameters. The fan operating line was controlled by downstream valves at the collector exit. Performance parameters were corrected to standard day conditions of a temperature of 288.15 K (518.67° R) and an atmospheric pressure of 101 kPa (760 mm Hg.).

Figure 3 shows a cross-sectional sketch of the fan stage as installed in the anechoic chamber. Also shown on Fig. 3 are some design param-

ters for the fan. An inlet with internal contours typical of flight inlets, but with a thicker lip to facilitate static testing was used for these tests. An acoustically-treated annular flow splitter with radial support vanes was installed downstream of the fan to guide and stabilize the flow as it expanded radially into the exhaust collector, and to attenuate any aft fan noise which might be reflected back toward the fan from the collector. The fan stage was externally driven by an electric motor. A photograph of the partially-assembled fan rotor is shown in Fig. 4.

Inflow Control Device

Figure 5 shows a cross-sectional sketch of the three variations of the NASA-Lewis inflow control device (ICD). The basic configuration described in Ref. 4, consisted of 5 cm (2 in.) thick honeycomb over a 40% open area screen and supported by a stronger, 70% open area screen. The second ICD configuration consisted of the addition of a 70% open area screen supported 10 cm (4 in.) inside of the basic structure. The study reported in Ref. 11 found such a downstream screen useful in combination with honeycomb/screen flow manipulators in reducing the turbulence intensities. Reference 7 reports the results of an experimental fan noise study for a similar ICD with a downstream screen supported 5 cm (2 in.) inside the basic structure. The Ref. 7 ICD was not tested without the inner screen in place.

The third ICD configuration adapted another experimental inflow control concept to the current ICD tests. This other inflow control concept consisted of an annular duct with a concentric bellmouth located at the flight inlet lip. Suction was applied to the annular duct in an attempt to simulate a forward flight condition. The suction was intended to modify the fan inflow in the area of the inlet lip to be more representative of flow with a low fan forward velocity, with an expected reduction of the rotor-inflow noise.

The third ICD configuration reported in this study and illustrated in Fig. 5 was formed by mating a portion of the annular flow duct to the back of the basic ICD with the inner screen liner in place. In this configuration it was possible to use aft suction to remove airflow which might otherwise enter the fan inlet from behind the highlight. It was thought that disturbances in the forward flow on the outside of the fan inlet or disturbances generated in negotiating the turn around the inlet lip would be superimposed on the inlet boundary layer, degrading the inlet flow near the fan tip, and possibly increasing the rotor-inflow noise. There was also concern that small irregularities in the attachment of the ICD to the fan inlet might induce inlet disturbances. Aft suction should eliminate this potential problem.

In the ICD study of Ref. 7, suction was applied to the inner surface of the inlet duct. The results of this study suggested that suction was effective in further reducing the blade passing tone with the ICD in place on the inlet.

Figure 6 is a photograph showing the ICD installed on the test fan in the anechoic chamber.

Acoustic Instrumentation

Far field acoustic data were acquired on a 7.6 m (25 ft) radius from 0° to 90° from the fan inlet axis (in 10° increments). Signals from the 0.64 cm (0.25 in.) microphones were recorded on magnetic tape for later narrow bandwidth spectral analysis. The output of this narrow bandwidth sound pressure level analysis was digitized and transmitted to a computer for further analysis. Using a computer reduction program, narrow bandwidth sound power level spectra were generated for the forward arc (0° to 90° from the fan inlet axis).

The b-7c microphone (seen in Fig. 1) was used to obtain continuous directivity results at a 6.1 m (20 ft) radius centered in the plane of the fan inlet highlight. The narrow bandwidth spectral analyzer was used to monitor the fundamental and first overtone levels for these boom traverses (80 Hz bandwidth).

III. Results and Discussion

Aerodynamic Results

The fan operating map (Fig. 7) shows the aerodynamic performance of the research fan as tested in the anechoic chamber.¹⁰ Most of the acoustic results presented in this paper are for the fan operation on the standard operating line.

Acoustic Results

Because of the high design speed of this research fan, most of the acoustic results discussed in this section will be for 60 and 70% of design fan speed. Above 70% design speed the rotor relative velocity is well into the supersonic region where inflow control has little effect on strong multiple pure tone generation associated with rotor blade leading edge shock waves. Since the research fan in this study was a cut-on design, inflow control was not expected to substantially reduce the fundamental blade passing tone levels if they were due to rotor-stator interaction. However, as the following results will show, rotor-inflow interaction noise still appears to be the dominant fundamental tone generation mechanism - even for the cut-on fan design.

Tests of the original aft suction concept showed little tone reduction without the addition of an ICD to condition the bulk of the inflow. The results implied that disturbed flow at the inlet lip and inlet duct boundary layer is not the major source for the rotor-inflow tone noise generation.

Sound power level spectral. Sound power level (PWL) spectra were calculated for the forward arc. Figure 8 shows PWL spectra for 60 and 70% design fan speed. Figure 8(a) compares PWL spectra at 60% design fan speed for the baseline fan stage without inflow control to spectra for the stage with the basic ICD, and to spectra for the configuration with the inner screen liner and aft suction. The basic ICD is seen to reduce the fundamental tone power level by about 8 dB. A further 4 dB reduction of the fundamental tone was realized by the addition of the inner screen liner

and aft suction. The first overtone levels (designated 2 x BPF on Fig. 8(a)) showed a small reduction with the basic ICD, but were reduced an additional 3 dB with the additional inflow control. The results for the basic ICD with the liner screen in place, but no aft suction were essentially the same as those for the basic ICD, and are not shown on this figure.

Figure 8(b) shows the same comparison for the fan operating at 70% of design speed. These results are similar to those of Fig. 8(a), showing considerable reduction of the fundamental tone level with the basic ICD, and further tone reduction with the addition of the inner screen and aft suction. Thus in the presence of the basic ICD to condition the bulk of the inflow, there is evidence that disturbances associated with forward flow on the outside of the fan inlet or with flow around the inlet lip are present to generate tone noise. This contrasts with the case cited above where without the ICD there was no effect of aft suction.

The rotor relative velocity is in the supersonic region at 70% design speed for this fan. In Fig. 8(b) there is evidence of the initial stages of multiple pure tone generation in the baseline (no inflow control) spectra at about 4 kHz and again between the fundamental and first overtone. These MPTs were essentially reduced to broadband levels in the spectra with inflow control. At 80% design fan speed the multiple pure tones were well established and essentially no difference was seen between the MPT levels for the baseline and inflow control cases. A similar observation on the effect of inflow control on suppressing MPT generation in the trans-sonic rotor tip speed range was reported in Ref. 4.

Sound pressure level directivity. Directivity results for the baseline fan and for the fan with inflow control are shown in Figs. 9 to 11. These tone levels were obtained from narrow bandwidth SPL spectra (80 Hz bandwidth) from the fixed, far field microphone signals and from the microphone boom signal.

The fixed-position directivity plot for the blade passing tone at 60% design fan speed is shown in Fig. 9(a). The baseline results show a directivity pattern that is typical for rotor-inflow interaction in which the energies of many acoustic radiation modes are combined with no particular modal pattern dominating the directivity. (See Ref. 12 for a discussion of the addition of acoustic modes.)

Essentially similar results are seen with the ICD with and without the inner screen liner. A lobed pattern begins to appear in the directivity with this level of inflow control, suggesting that a limited number of driving modes now control the directivity. However, with the addition of aft suction a different lobed pattern emerges at a somewhat further reduced level. As was previously discussed, the aft suction was expected to greatly reduce inflow disturbances originating from any disturbances introduced by the ICD-fan inlet interface as well as disturbances from forward flow on the outside of the inlet merging with the inflow boundary layer. This change in the lobed pattern with the addition of aft suction gives evidence for the existence of such local flow problems with the other ICD configurations.

The directivity with maximum inflow control (ICD with aft suction) does not show a strongly-lobed structure. This suggests that the residual fan fundamental tone is not controlled by a few rotor-stator interaction generated modes for this fan speed and rotor-stator spacing (1.6 rotor chords).

The continuous-sweep SPL directivity results from the microphone boom signal corresponding to the fixed point results of Fig. 9(a) are shown in Fig. 9(b). The results for the ICD with screen liner were omitted for clarity. Distinct lobes in the directivity structure for the base ICD results are quite evident in this figure.

The blade passing tone SPL directivity results at 70% design fan speed (Figs. 10(a) and (b)) show essentially the same trends as were observed for 60% design fan speed. The remaining lobed structure in the directivity with maximum inflow control suggests a tone contribution from rotor-stator interaction modes.

Directivity plots for the first overtone (Figs. 11(a) and (b)) show a modest tone reduction at all angles with the maximum inflow control configuration. The reduction of the first overtone with inflow control is considerably less than that observed for the fundamental tone. The results for the intermediate inflow control configurations fell between these two curves.

Tone sound power level. The fan blade passing tone sound power level is shown as a function of fan speed in Fig. 12. Inflow control is seen to be very effective in reducing this tone level at 60 and 70% design fan speed. The effectiveness of inflow control is greatly reduced at 80% design speed and above, where the rotor relative velocity is well into the supersonic range. Again, the addition of the inner screen to the ICD did not appreciably reduce the tone level.

The approximately 3 dB reduction of the tone level with inflow control at higher fan speeds is due to a reduction in the rotor-inflow interaction noise at angles nearer the fan axis. For example, Fig. 13 compares the blade passing tone SPL directivities for the baseline and maximum inflow control configurations at 90% design fan speed. The directivity pattern associated with the rotor-alone tone generation at supersonic tip speeds peaks near 60° from the fan inlet. No tone reduction was observed with inflow control at 60° to 90° from the inlet axis, where the levels were controlled by the rotor-alone field. However, inflow control does reduce the tone level at forward angles where rotor-inflow dominates. The net results are the small tone power reductions observed with inflow control at supersonic blade tip speeds.

The choke operating line results of Fig. 14 suggest that the moderate inflow control afforded by the basic ICD is more effective in reducing the blade passing tone for fan operation on the choke line than for operation on the standard line at 70 and 80% design fan speed. Fan operation on the choke operating line results in a higher axial velocity for a given fan speed, thus slightly reducing the rotor-inflow incidence angle and rotor loading. These results suggest that such changes in the rotor operating condition may influence the

sensitivity of the blade passing tone level to inflow conditions.

Figure 15 shows the first overtone PNL as a function of fan speed for the baseline and maximum inflow control configurations. Inflow control resulted in about a 5 dB reduction in the overtone at 60% design fan speed, with decreasing effect with increasing fan speed. Thus, the first overtone is controlled by rotor-inflow interaction at lower fan speeds, with rotor alone tone generation becoming more significant with increasing fan speed.

IV. Summary of Results

1. Rotor-inflow interaction appears to be a stronger source than rotor-stator interaction for the forward radiated blade passing tone as evidenced by the effectiveness of inflow control with this cut-on fan at a 1.6 rotor chord rotor-stator spacing.

2. Aft suction used in conjunction with an inflow control device was beneficial in further reducing forward-radiated blade passing tone levels. This suggests that disturbances either in the forward flow on the outside of the fan inlet or associated with flow around the inlet lip may be an important noise generating mechanism. The disturbances could also come from irregularities at the mating surfaces between the ICD and the inlet outer wall.

3. The sensitivity of the fan blade passing tone level to inflow conditions is reduced when the rotor incidence angle is decreased by operation on the choke operating line.

References

1. Feiler, C. E. and Groeneweg, J. F., "Summary of Forward Velocity Effects on Fan Noise," NASA TM-73722, 1977; AIAA Paper 77-1319, Oct. 1977.
2. Dietrich, D. A., Heidmann, M. F., and Abbott, J. M., "Acoustic Signatures of a Model Fan in the NASA-Lewis Anechoic Wind Tunnel," AIAA Paper 77-59, Jan. 1977.
3. Hanson, D. A., "Measurements of Static Inlet Turbulence," AIAA Paper 75-467, Mar. 1975.
4. Woodward, R. P., Wazyniak, J. A., Shaw, L. M., and MacKinnon, M. J., "Effectiveness of an Inlet Flow Turbulence Control Device to Simulate Flight Fan Noise in an Anechoic Chamber," NASA TM-72855, 1977.
5. Cocking, B. J., and Ginder, R. B., "The Effect of an Inlet Flow Conditioner on Fan Distortion Tones," AIAA Paper 77-1324, Oct. 1977.
6. Jones, W. L., McArdle, J. G., and Homyak, L., "Evaluation of Two Inflow Control Devices for Flight Simulation of Fan Noise Using a JT15D Engine," NASA TM-79072, 1979; AIAA Paper 79-0654, Mar. 1979.
7. Kantola, R. A. and Warren, R. E., "Reduction of Rotor-Turbulence Interaction Noise in Static Fan Noise Testing," AIAA Paper 79-0656, Mar. 1979.
8. Wazyniak, J. A., Shaw, L. M., and Essary, J. D., "Characteristics of an Anechoic Chamber for Fan Noise Testing," NASA TM X-73555, 1977.
9. Erwin, J. R. and Heldenbrand, R. W., "Advanced Acoustic and Aerodynamic 20-Inch Fan Program," AiResearch Mfg. Co., Phoenix, AZ, AIRESEARCH-75-211789, Dec. 1977. (NASA CR-135093)
10. Lucas, J. G., Woodward, R. P., and MacKinnon, M. J., "Forward Acoustic Performance of a Shock-Swallowing High Tip Speed Fan," NASA TP , 1980.
11. Loehrke, R. I. and Nagib, H. M., "Control of Free Stream Turbulence by Means of Honeycombs: A Balance Between Suppression and Generation," Journal of Fluids Engineering, Vol. 98, Sep. 1976, pp. 342-353.
12. Heidmann, M. F., Saule, A. V., and McArdle, J. G., "Analysis of Radiation Patterns of Interaction Tone Generated by Inlet Rods in the JT15D Engine," AIAA Paper 79-0581, Mar. 1979.

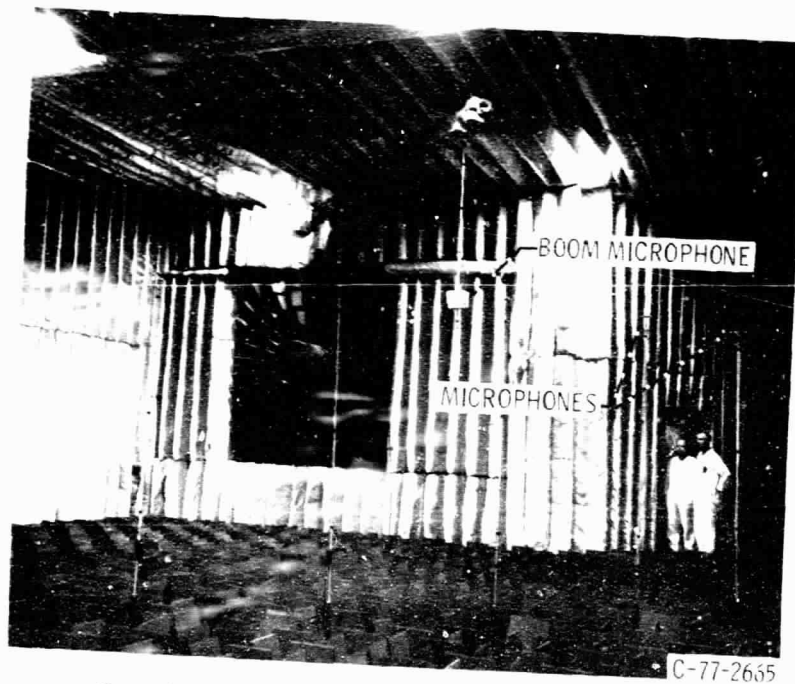
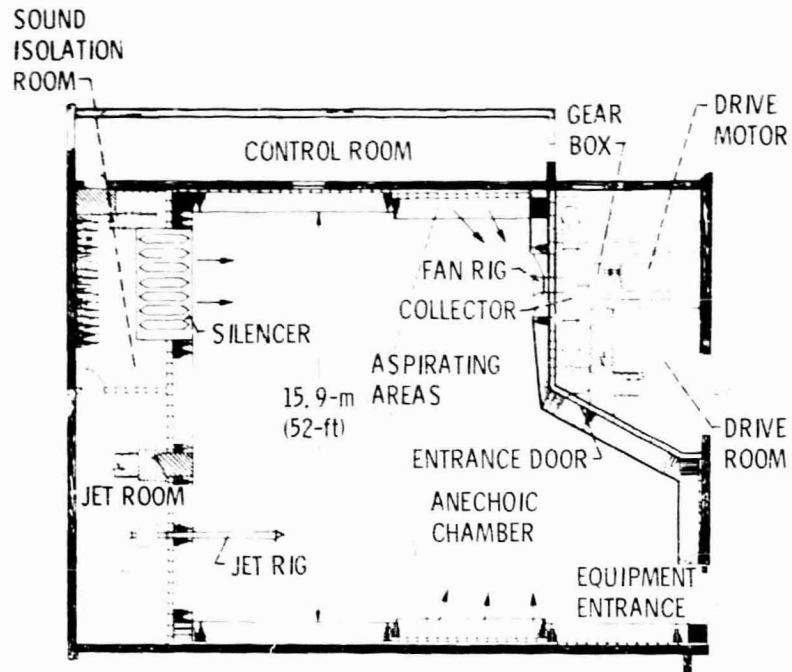
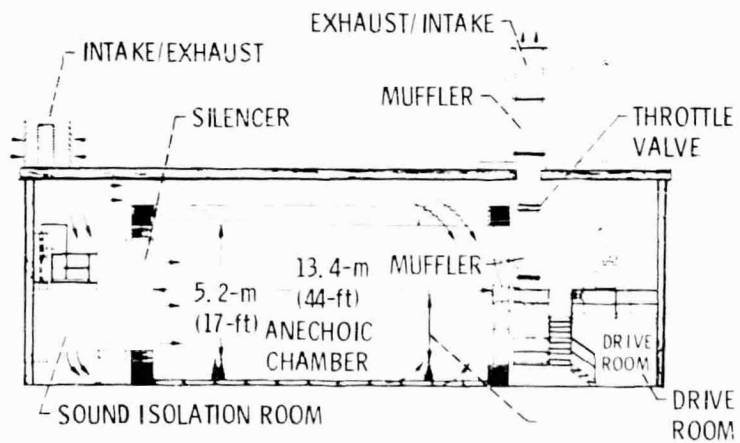


Figure 1. - Research fan installed in anechoic chamber.

[Faint, illegible handwritten text]



(a) NOISE FACILITY FLOOR PLAN.



(b) NOISE FACILITY ELEVATION VIEW.

Figure 2. - Anechoic chamber.

DESIGN PARAMETERS

ROTATIVE SPEED	18 300 rpm
TIP SPEED	487.7 m/sec (1600 ft/sec)
STAGE TOTAL PRESSURE RATIO	1.5
MASS FLOW	32.5 kg/sec (71.7 lbm/sec)

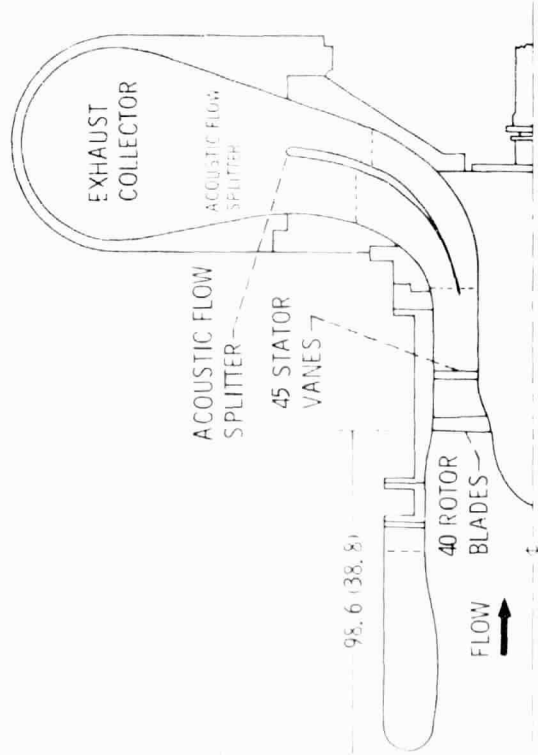
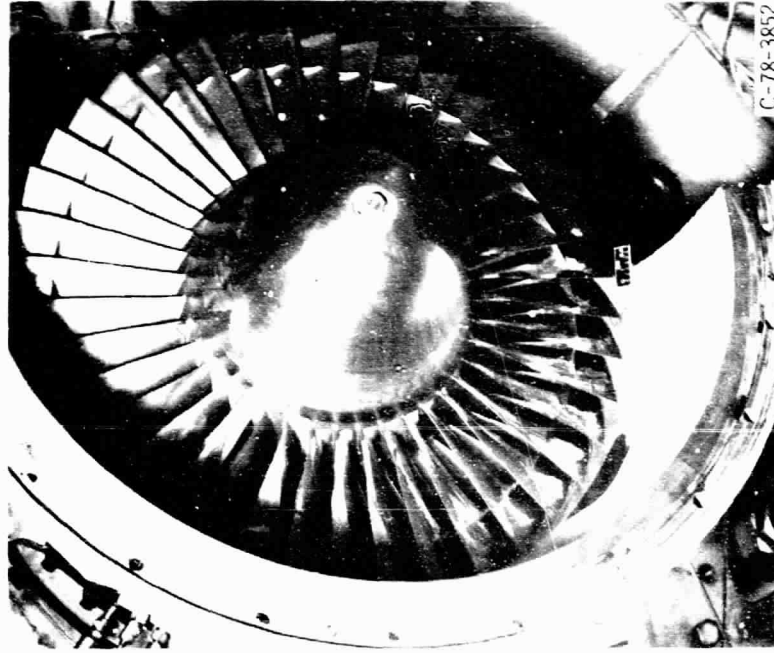


Figure 3. - Cross-sectional view of the research fan in the anechoic chamber and table of design parameters (dimensions are in cm (in.)).



C-78-3852

Figure 4. - View of partially assembled fan stage showing rotor blading

ICD WITH INNER LINER AND AFT SUCTION

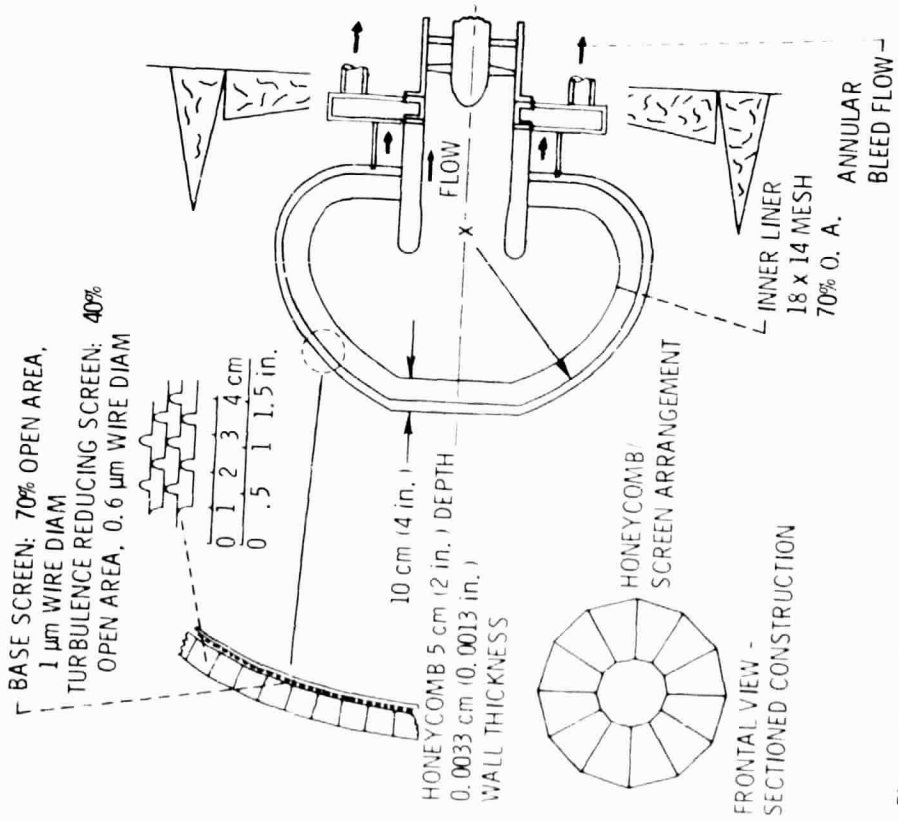
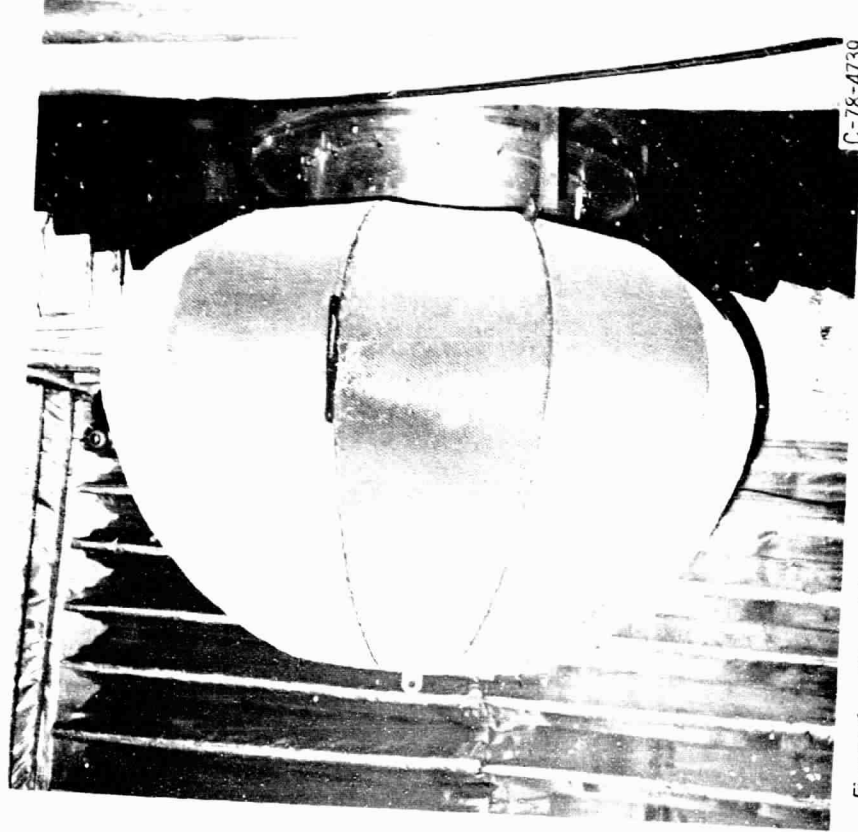


Figure 5. - Inflow control device showing inner screen liner and adaptation of annular flow for aft suction.



C-78-4739

Figure 6. - View of the inflow control device installed in the LeRC anechoic chamber.

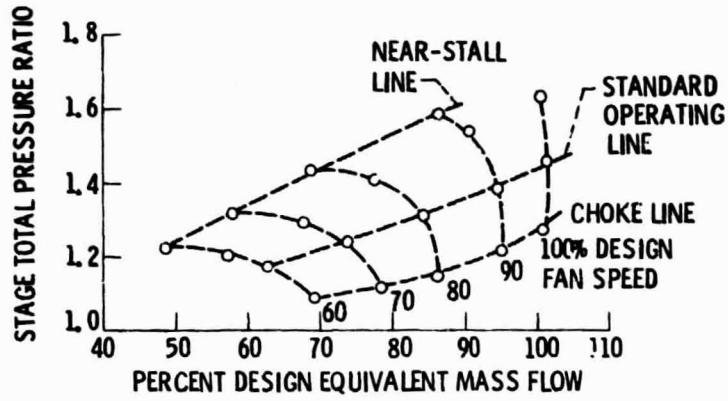


Figure 7. - Fan operating map.

- BASELINE - NO INFLOW CONTROL
- - - WITH INFLOW CONTROL DEVICE (ICD)
- · · WITH ICD, LINER, AND AFT SUCTION

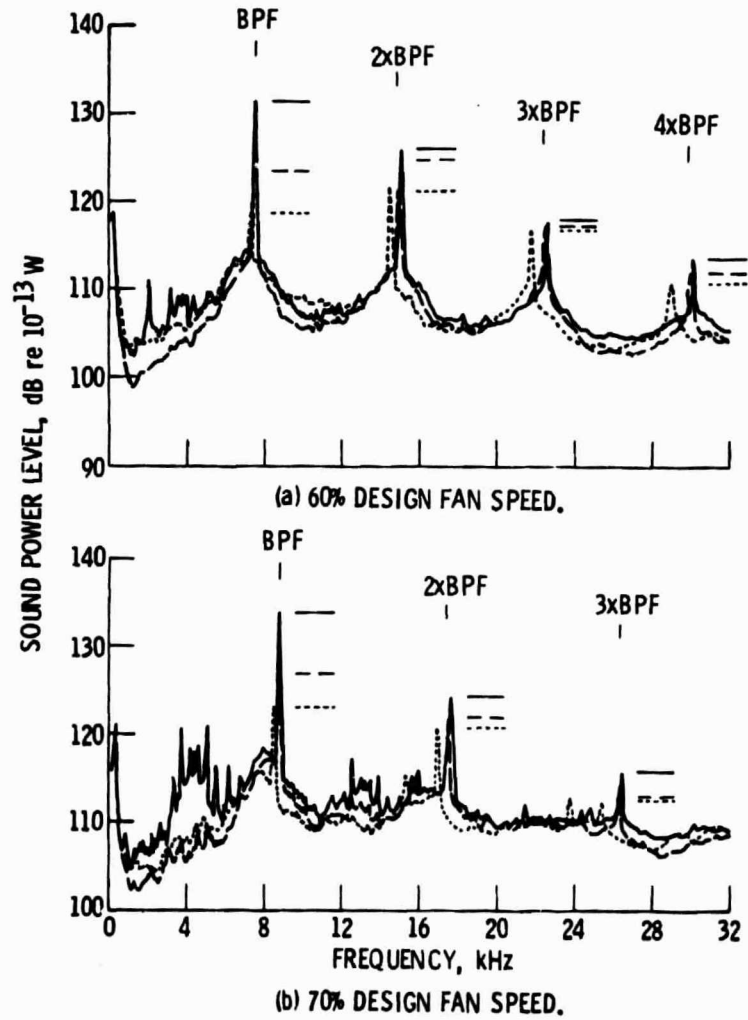


Figure 8. - Sound power level spectra (80 Hz bandwidth), standard operating line.

- BASELINE, NO INFLOW CONTROL
- WITH INFLOW CONTROL DEVICE (ICD)
- ◇ WITH ICD AND INNER SCREEN LINER
- △ WITH ICD, LINER, AND AFT SUCTION

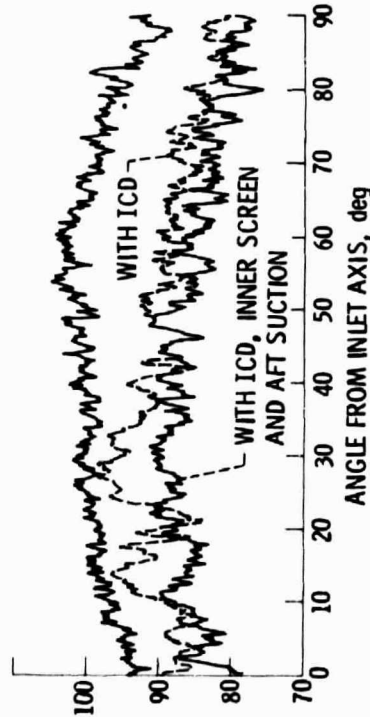
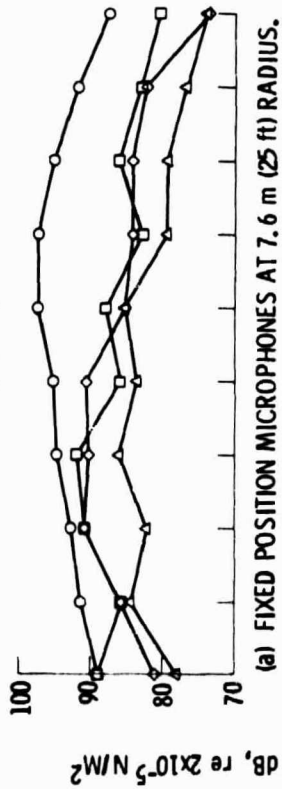


Figure 9. - Blade passing tone sound pressure level directivity, 60% design fan speed, standard operating line, 80 Hz bandwidth.

- BASELINE, NO INFLOW CONTROL
- WITH INFLOW CONTROL DEVICE (ICD)
- ◇ WITH ICD AND INNER SCREEN LINER
- △ WITH ICD, LINER, AND AFT SUCTION

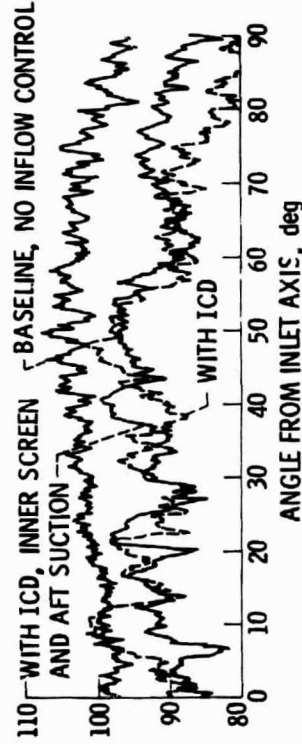
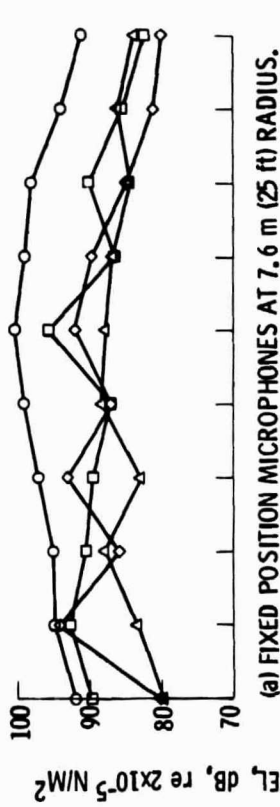


Figure 10. - Blade passing tone sound, pressure level directivity, 70% design fan speed, standard operating line, 80 Hz bandwidth.

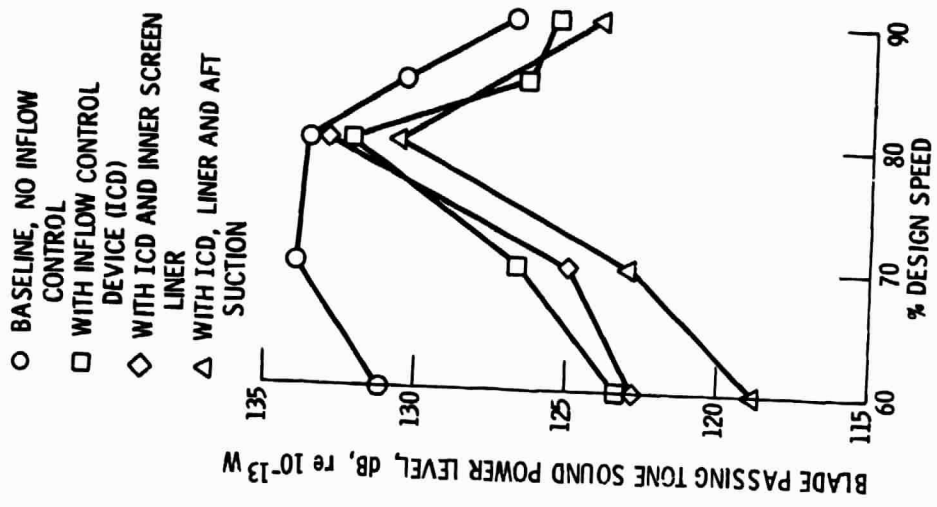


Figure 12. - Narrowband blade passing tone sound power level as a function of fan speed. Standard operating line, 80 Hz bandwidth.

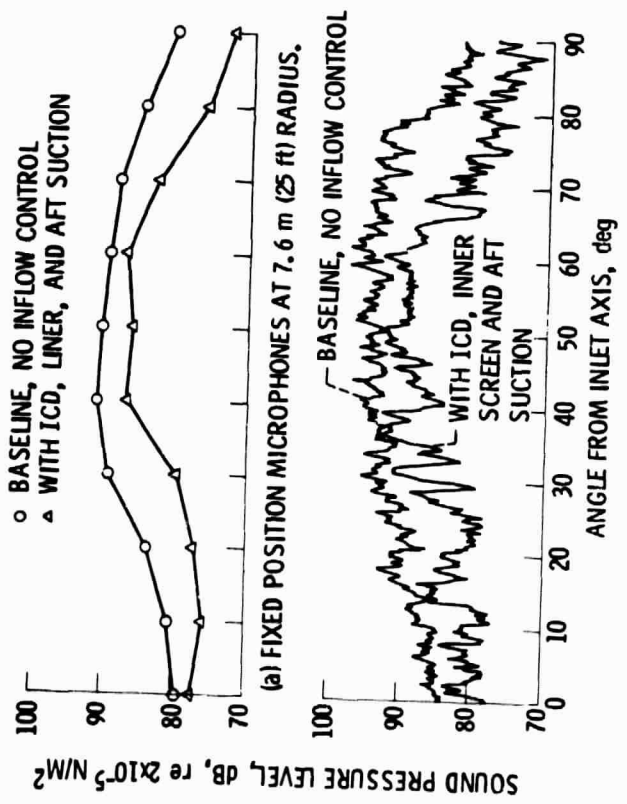


Figure 11. - First overtone (2x BPF) sound pressure level directivity, 60% design fan speed, standard operating line, 80 Hz bandwidth.

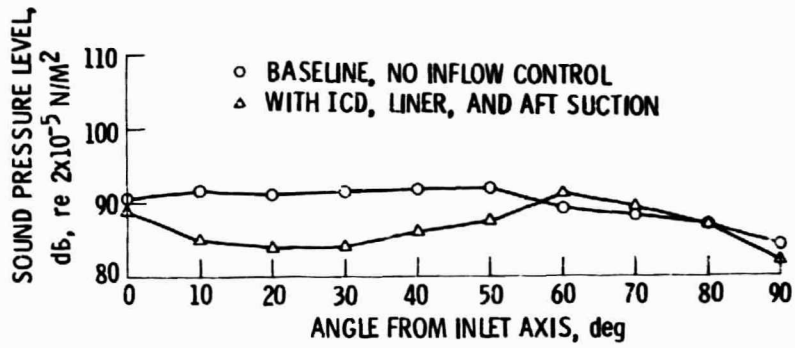


Figure 13. - Blade passing tone SPL directivity at 7.6 m (25 ft) radius. 90% design fan speed, standard operating line.

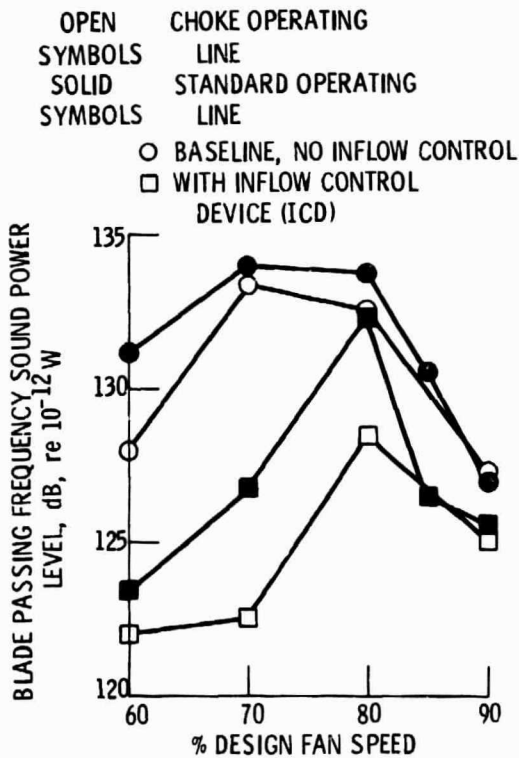


Figure 14. - Narrowband blade passing tone sound power level as a function of fan speed, 80 Hz bandwidth.

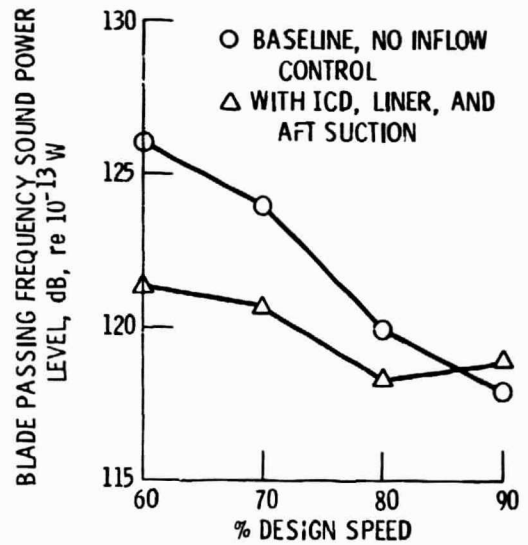


Figure 15. - Narrowband 1st overtone sound power level as a function of fan speed. Standard operating line, 80 Hz bandwidth.